Nitrogen Heterocyclic Compounds as Corrosion Inhibitors for C-Steel in Aqueous Media

Amira E.Ali [1] , Ahmed El- Mekabaty[1] , Gamila E. Badr [1] , Abd El-Aziz S. Fouda [1,]*

1 Chemistry Department, Faculty of Science, Mansoura University, Mansoura-35516, Egypt;

* *Correspondence*: asfouda@hotmail.com.

Abstract: The dissolution of CS in corrosive medium which is half molar of sulfuric acid has been studied by using chemical methods such as mass loss calculation at different temperature and Non-chemical methods such as PP and EIS methods .Also,the dissolution of CS was confirmed by surface examination techniques such as FT-IR.

1. Introduction:

Carbon steel is used in various industries such as low-carbon steel is the metal of choice for building frames in commercial, government and residential buildings. Bridges, steel piping and many automotive parts are also made from low-carbon steel. Smaller products made of low carbon steel include nails, wires, pipes and chain. High-carbon steel, with its even greater durability, is often used in cutting tools, springs, coils, wrenches, hammers, and other types of tools and equipment used in the building process.We used sulfuric acid as corrosive media due to its importance due to it used in many industries processes such as Fertilizers, Pharmaceuticals, Gasoline , Automobile batteries , Paper bleaching ,Sugar bleaching ,Water treatment ,Sulfonation agents and Steel manufacturing [1]. Both anodic and cathodic effects are sometimes observed in the presence of organic inhibitors but, as a general rule, organic inhibitors affect the entire surface of a corroding metal when present in sufficient concentration. Organic inhibitors usually designated as 'film-forming', protect the metal by forming a hydrophobic film on the metal surface.The effectiveness of these inhibitors depends on the chemical composition, their molecular structure, and their affinities for the metal surface [2] Because film formation is an adsorption process, the temperature and

pressure in the system are important factors.Organic inhibitors will be adsorbed according to the ionic charge of the inhibitor and the charge on the surface. Cationic inhibitors, such as amines, or anionic inhibitors, such as sulfonates, will be adsorbed preferentially depending on whether the metal is charged negatively or positively. The strength of the adsorption bond is the dominant factor for soluble organic inhibitors.

2. Experimental

2.1 Material and methods

2.1.1. Chemical composition of CS:

Table1. Chemical composition of CS:

Element	C	Mn	P	S	Fe
Mass (%)	0.610	0.754	0.013	0.254	Balance

2.1.2. Corrosive media (Sulfuric acid):

Approximately 10 M sulfuric acid solution was prepared. The concentrations of the acid were checked by titration of an appropriately diluted portion with standard solution of sodium carbonate. From these stock dilute solutions exactly 0.5 M solutions were prepared by dilution which was used throughout all the experiments for the preparation of solutions.

2.1.3. Organic solvents:

Ethanol (99%) and DMF.

2.1.4. Inhibitor

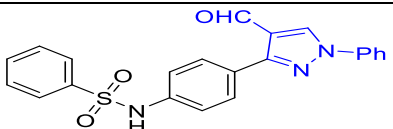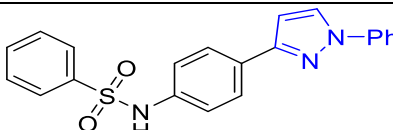1- **N-(4-(4-Formyl-1-phenyl-1H-pyrazol-3-yl)phenyl)benzenesulfonamide.**

To a cold solution of phenylhydrazone (1.46 g, 4 mmol) in DMF (10 mL), phosphorus oxychloride (0.55 mL, 6 mmol) was added dropwise with stirring for 15 min. Stirring was continued for one hour at room temperature. The mixture was heated at 70-80°C for 2 h, then cooled at 25°C and poured onto ice-cold water. A saturated solution of K_2CO_3 was added to neutralize the mixture. The 4-formylpyrazole was filtered off, washed extensively with water and recrystallized by boiling in ethyl alcohol.

2-N-(4-(1-phenyl-1H-pyrazol-3-yl)phenyl)benzenesulfonamide.

Phenylhydrazine (0.01 mol) was added to a solution of enaminone (3.30 g, 0.01 mol) in 30 mL glacial acetic acid and refluxed for 6 h. The reaction mixture (after cooling) was poured onto crushed ice and the solid formed was filtered off and recrystallized by heating in ethyl alcohol.

Table 2 : Chemical structure of inhibitors :

Inhibitors	Structure	Mol.wt, Mol Formula	Names
A		403.46 , $C_{22}H_{17}N_3O_3S$	N-(4-(4-Formyl-1-phenyl-1H-pyrazol-3-yl)phenyl)benzenesulfonamide.
B		375.45 , $C_{21}H_{17}N_3O_2S$	N-(4-(1-phenyl-1H-pyrazol-3-yl)phenyl)benzenesulfonamide.

2.1.5. Chemical methods

2.1.5.1. Mass loss measurements (ML):

Before starting the measurements, the coupons must be mechanically treated with emery sheets of different grades (400-2000) which abraded to finish a mirror then washed them with acetone and distilled water finally dried with filter paper and weighted using electrical balance [3]. In this method, CS pieces with dimension (20 x 20 x 2 mm) are used .By the aid of glass hooks , the test specimens were hanged into a volume of 100 ml of electrolyte solutions so that the whole surface of CS sample is completely immersed and uniformly attacked by corrosive solution. After interval time of immersion (30 min), the samples get out from the test solution, washed with bi-distilled water , dried and weighted . The ML was determined at the ending of the process and in the existence of various doses of inhibitors.The following equations were used to calculate the corrosion rates (CR) .

$\theta = CR - CR_{(i)} / CR$ (1)

$C.R = \frac{M}{A \, X \, t}$ (2)

$\% IE = \theta \times 100$ (3)

Where M is the weight loss (mg) , A is the area (cm^2) , t is the time (min).

2.1.5.2- Electrochemical method

For electrochemical methods, three different electrodes are combined together in a glass cell

a- Working Electrode:

CS acts as (WE). The CS surface polished with emery papers before starting the process and degreased in acetone and dried then immersed in the electrolyte solution.

b- Reference Electrode:

The reference electrode is Silver / Silver Chloride electrode. It put close to working electrode to minimize the potential drop.

c- Auxiliary Electrode:

It made from platinum wire.

The electrochemical measurements were done by Potentiostat-Galvanostat-ZRA analyzer and the analysis of the data given from tests had achieved by E-chem Analyst 5.5 software.

2.1.5.3. Surface examination techniques:

The morphology of CS surface is examined and studied by different techniques[11] :

a- FT-IR:

CS specimens were examined with Thermo Fisher Scientific Waltham, MA, USA) device [4].

3.Results and Discussion

3.1. mass-loss l method.

The variation of CR and % IE with different concentrations of the studied compounds (10 $x10^{-6}$ – 50 $x10^{-6}$ M) at different temperatures (25- 45°c) is represented in Table(1). Corrosion parameters derived from ML method are given in Table (2) . From which a reduction in CR is noticed when the concentration of studied inhibitors increase. In general, inhibitor molecules retard the corrosion reactions by covering the surface area for attack by the corrosive media and blocking the sites of corrosion.
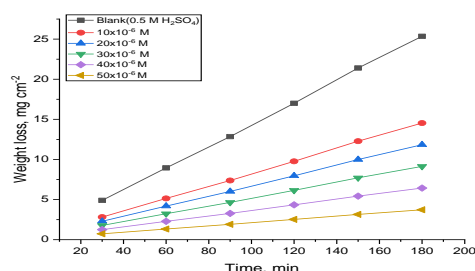

Fig 1. Weight loss-time curves for CS dissolution in half molar of H_2SO_4 in the non-existence and existence of various doses of compound (A) at 25°C.
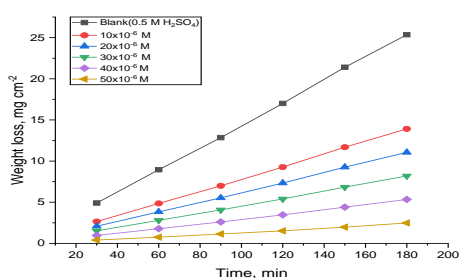

Fig 2. Weight loss-time curves for CS dissolution in half molar of H_2SO_4 in the existence and non-existence of various doses of compound (B) at 25°C.

Table1. Effect of temperature on corrosion rate

Compound	Temp,℃	Corrosionrate,(CR) (mg cm^{-2}min^{-1})
Blank	25	0.141
	30	0.181
	35	0.254
	40	0.327
	45	0.369

Table 2. Variation of inhibition efficiency (%IE) of compound (A) from weight loss calculation at two hours dispersion in 0.5 M H_2SO_4 at different temperatures from (25-45)^{O}C.

Conc, M	Temp, ℃	Corrosionrate,(CR) (mg cm^{-2}min^{-1})	0	%IE
10 x10^{-6}	25	0.0275	0.827	82.7
	30	0.0458	0.824	82.4
	35	0.054	0.791	79.1
	40	0.1026	0.772	77.2
	45	0.1197	0.765	76.5
20 x10^{-6}	25	0.0246	0.831	83.1
	30	0.042	0.83	83
	35	0.052	0.80	80
	40	0.1006	0.779	77.9
	45	0.1181	0.767	76.7
30 x10^{-6}	25	0.023	0.843	84.3
	30	0.0399	0.837	83.7
	35	0.0502	0.808	80.8
	40	0.0992	0.785	78.5
	45	0.1157	0.773	77.3
40 x10^{-6}	25	0.0227	0.847	84.7
	30	0.039	0.838	83.8
	35	0.0468	0.814	81.4
	40	0.094	0.787	78.7
	45	0.112	0.774	77.4
50 x10^{-6}	25	.021	0.852	85.2
	30	0.035	0.85	85
	35	0.046	0.816	81.6
	40	0.064	0.793	79.3
	45	0.078	0.779	77.9

Table 3. Variation of inhibition efficiency (%IE) of compound (B) from weight loss calculations at two hours dispersion in 0.5 M H_2SO_4 at different temperatures from (25-45)^{O}C

Conc, M	Temp, ℃	Corrosionrate,(CR) (mg cm^{-2}min^{-1})	0	%IE
10 x 10^{-6}	25	0.0186	0.878	87.8
	30	0.0341	0.855	85.5
	35	0.0476	0.822	82.2
	40	0.0725	0.802	80.5
	45	0.1057	0.768	76.8
20 x10^{-6}	25	0.0172	0.881	88.1
	30	0.0327	0.856	85.6
	35	0.0443	0.832	83.2
	40	0.0692	0.820	82
	45	0.1023	0.778	77.8
30 x10^{-6}	25	0.017	0.892	89.2
	30	0.032	0.86	86
	35	0.041	0.846	84.6
	40	0.067	0.821	82.1
	45	0.1076	0.780	78
40 x10^{-6}	25	0.0148	0.904	90.4
	30	0.028	0.865	86.5
	35	0.0376	0.857	85.7
	40	0.065	0.829	82.9
	45	0.1	0.793	79.3
50 x10^{-6}	25	0.013	0.911	91.1
	30	0.021	0.879	87.9
	35	0.031	0.866	86.6
	40	0.0606	0.83	83
	45	0.099	0.796	79.6

3.1.1. Adsorption isotherm of CS

The adsorption isotherm is useful for determining the nature and form of corrosion inhibition mechanism. When the inhibitor adsorbed on the metal ,it adsorbed with its surface by chemical or physical reaction [5].There are many factors which affect the adsorption process such as the inhibitor configuration , the kind of the metal , the surface nature , the pH of the surrounded corrosive media and its type and the temperature process . The adsorption process may illustrate by many adsorption isotherm of CS.In this process the Temkin isotherm is the more appropriate model to explain the adsorption of inhibitors on CS surface. The expression of Temkin model is :

$$\Theta = \frac{2.303}{a} \log K_{ads} + \frac{2.303}{a} \log C_{inh} \quad (4)$$

Where Θ is the surface coverage , C_{inh} is the dose of inhibitor , K_{ads} is the constant of equilibrium adsorption and (a) is parameter of molecular interaction.

The K_{ads} is related with the Gibbs free energy by this formula:

$$\text{Log } K_{ads} = - \log 55.5 - \frac{\Delta G^{\circ}_{ads}}{2.303 \, RT} \quad (5)$$

By applying van't Hoff equation , we calculate the enthalpy and standard entropy parameters.

$$\text{Log } K_{ads} = \frac{-\Delta H^{\circ}_{ads}}{2.303 \, RT} + \text{constant} \quad (6)$$

$$\Delta G^{\circ}_{ads} = \Delta H^{\circ}_{ads} - T\Delta S^{\circ}_{ads}$$

The resulted table indicated that ,

1-The process is spontaneous and the adsorption is physical due to the negative sign of Gibbs free energy and its value close to 20 kJ mol^{-1}.

2-The adsorption is exothermic and pysisorption due to the negative sign of enthalpy.
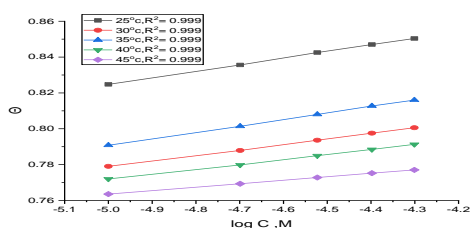

Fig 3. Temkin Adsorption isotherm curves of compound (A) on CS at different temperatures in half molar of H_2SO_4.
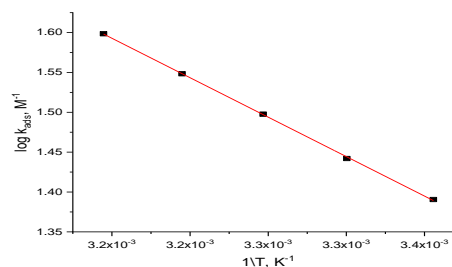

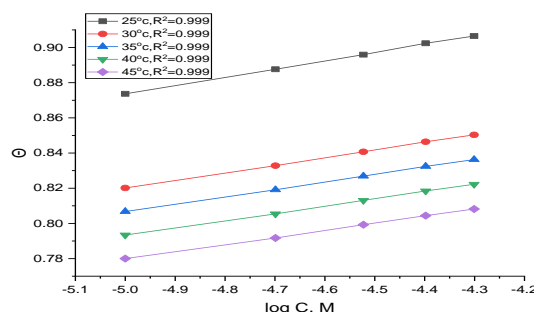**Fig4.** (1/T against log K_{ads}) curves presence and non-existence of various doses of compound (A).

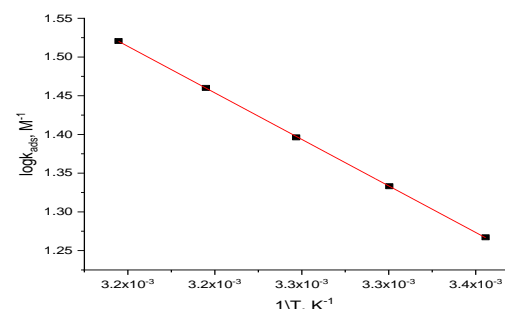**Fig5.** Temkin Adsorption isotherm curves of compound (B) on CS at different temperatures in half molar of H_2SO_4

Figure 6. (1/T against log K_{ads}) curves presence and non-existence of various doses of compound (B).

Table 4. Data of thermodynamic adsorption parameters.

Inhibitor	Temp k	K_{ads}	$-\Delta G^{\circ}_{ads}$	$-\Delta H^{\circ}_{ads}$	$-\Delta S^{\circ}_{ads}$
A	298	44.4	19.4	13.9	18.5
	303	31.9	18.8		16.2
	308	29.8	19		16.5
	313	27.2	19.1		16.6
	318	26.2	19.3		17
B	298	34.3	18.7	23.4	15.7
	303	247.7	18.5		16.1
	308	24.2	18.4		16.2
	313	23.1	18.6		15.3
	318	17.9	18.2		16.3

3.1.2. Activation thermodynamic parameters of corrosion process:

The mechanism of interaction among the CS surface and the inhibitors molecules illustrate by the activation parameters [6-12]. Equations (7&8) are Arrhenius and transition –state equation which used to calculate the activation thermodynamic parameters of CS corrosion without and with inhibitors in 0.5 MH_2SO_4 at (25-45°c).

$$K_{corr} = A \exp(-E_a^* / RT) \qquad (7)$$

$$K_{corr} = RT/Nh \exp(\Delta S^*/R) \exp(-\Delta H^* /RT) \ (8)$$

Where E_a^* is the activation energy , ΔH^* is the activation enthalpy , ΔS^* is entropy of activation , R indicated to gas constant ,N Avogadro's number and h plank constant .

From the table, it was shown that:

1-The values of activation energy increase with increasing concentration of inhibitor .This indicate that physisorption of the inhibitor.

2-The positive sign of activation entropy revealed to endothermic reaction.

3-The activation entropy has negative values, indicating that reduce in disorder from going from reactants to activated complex.
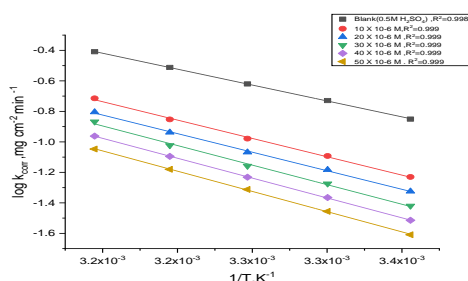

Fig7. Arrhenius plots of CS in half molar of H_2SO_4 in the non- existence and existence of various concentration of compound (A).
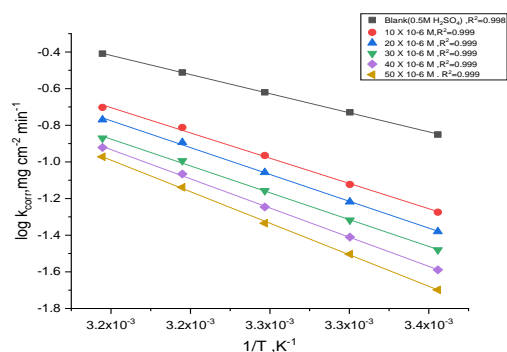

Fig8. Arrhenius plots of CS in half molar of H_2SO_4 in the non-existence and existence of various concentration of compound (B).
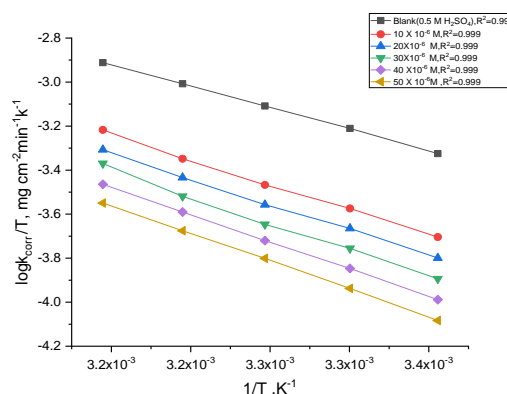

Fig9. Transition state plots of CS in half molar of H_2SO_4 in the non-existence and existence of various concentration of compound (A).
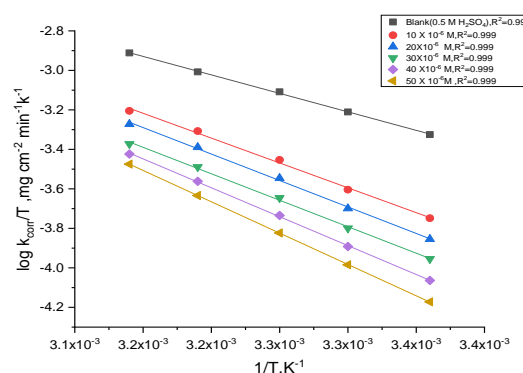

Fig10. Transition state plots of CS in half molar of H_2SO_4 in the non-existence and existence of various concentration of compound (B).

Table 5. Activation parameters of the dissolution of CS in 0.5 M H_2SO_4 in the non-existence and existence of different concentration of organic compounds.

Compound	[inh] M	E_a^* KJ mol^{-1}	ΔH^* KJ mol^{-1}	$-\Delta S^*$ Jmol^{-1}K^{-1}
Blank	0	39.7	37.1	199.1
A	10 x 10^{-6}	57.2	52.4	179
	20 x 10^{-6}	58.2	53.4	164.3
	30 x 10^{-6}	58.5	53.7	154.3
	40 x10^{-6}	58.6	54	141.5
	50 x 10^{-6}	59.6	54.7	137.7
B	10 x 10^{-6}	51.5	49.2	180.4
	20 x 10^{-6}	52.8	51.4	154.4
	30 x 10^{-6}	57	52.6	137.6
	40 x10^{-6}	60.9	57.7	126.2
	50 x 10^{-6}	62.5	60.9	120.3

3.2. Electrochemical Methods:

3.2.1. Potentidynamic polarization (PP) measurements:

By using the following equations:

% IE = θ x 100 = $[1-\frac{i_{corr}}{i^0_{corr}}]$ x 100 (9)

Where i_{corr} and i^o_{corr} are the corrosion currents in the existence and non-exist of the investigared

Fig .showed the PP curves of CS in the non-exist and exist of the compounds and from them we can noted that both cathodic and anodic reactiond are shifted to the positive and negative direction.

From the table (6) ,It was shown:

1-The corrosion current decreases by the increment of the concentration of investigated compounds.

2-CR decreased by added more of the compounds dose.

3-The investigated compounds act as mixed kind inhibitors which inhibit both anodic and cathodic reactions by blocked its active sites on the surface of the metal.

3.2.2. Electrochemical impedance spectroscopy measurements :

Electrochemical impedance method (EIS) occurred at OCP with applied frequency of (0.2Hz -100kHz) and the voltage was 10 mv . The data of Rct are used to determine the (%IE) as in equation (10) .

% IE = $\frac{R_{ct(inh)}-R_{ct}}{R_{ct(inh)}}$ x 100 (10)

Where R_{ct} and $R_{ct(inh)}$ are the charge transfer resistances in the absence and existence of the inhibitors, respectively.

Figures [13-17] represent the Nyquist and Bode curves for the CS dissolution in the presence and absence of different doses of investigated extracts in 0.5 M H_2SO_4 .The Nyquist plots have a semicircle shape and its diameter increased by increment the inhibitor dose but the Bode curves contain two loops connected to each other .
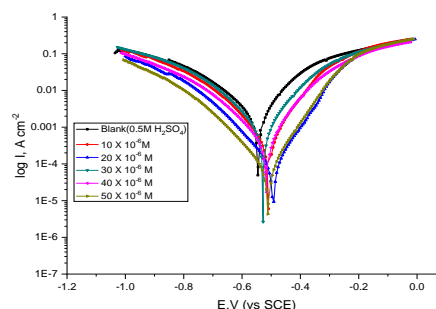

Figure11.PP plots of CS in the non-existence and existence of altered doses of compound (A) at 25°C.
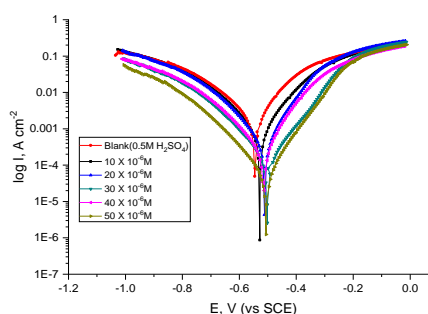

Figure12.PP plots for CS in the non-existence and existence of altered doses of compound (B) at 25°C

Table 6.electrochemical parameter for CS in 0.5MH_2SO_4 for existence and non-existence of various doses of inhibitors

Compound	[Inh] M	-E_corr mv vs SCE		βc mVdec-1	βa mVdec-1	k_corr mpy	θ	%IE
Blank	0.5	549	756	228.2	71.90	345.4	--	--
A	10 X 10^{-6}	528	149	153	52	66	0.803	80.3
	20 X 10^{-6}	519	125	145	45.7	60.70	0.835	83.5
	30 X 10^{-6}	511	100	140	46.9	52.85	0.867	86.8
	40 X 10^{-6}	508	95	138	46	50.85	0.874	87.4
	50 X 10^{-6}	503	83	132	42.7	37	0.89	89
B	10 X 10^{-6}	528	528	147	59.5	31	0.921	92.1
	20 X 10^{-6}	515	515	144	56	28.53	0.926	92.6
	30 X 10^{-6}	514	514	138	44.3	27.49	0.938	93.8
	40 X 10^{-6}	508	508	135	34.1	20.09	0.946	94.6
	50 X 10^{-6}	506	506	132	30	18	0.96	96

From the table,It was shown :

1-Rct increases by increasing the doses of inhibitors and the corrosion of the metal lowered due to the inhibitor's adsorption on the CS surface.

2-The capacitance of double layer decreased by increasing the inhibitors doses .

3-The surface coverage area and inhibition efficiency increased by increasing doses of invstigated inhibitors as the attendance of the adsorbed layer on the metal.
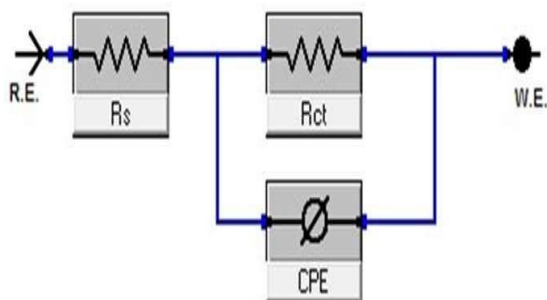

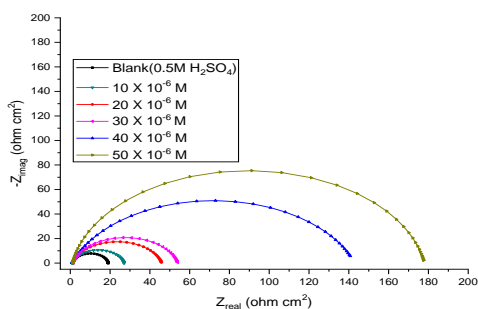**Fig13:** Circuit model used to match experimental EIS

Fig 14. The Nyquist plots for the dissolution of CS in half molar of H_2SO_4 in the existence of various doses of compound (A) at 25^oC.

Fig 15. Bode plots for the dissolution f CS in half molar of H_2SO_4 in thexistence and non-existence of various concentration of compound (A) at 25 ^{o}C.

Fig16. The Nyquist plots for the dissolution of CS in half molar of H_2SO_4 in the existence and non-existence of various concentration of compound (B) at 25 ^{o}C.
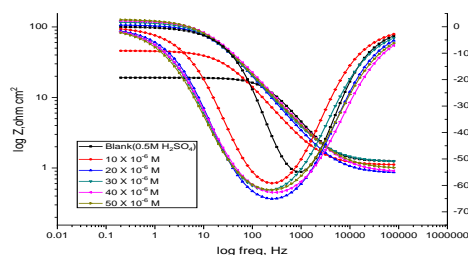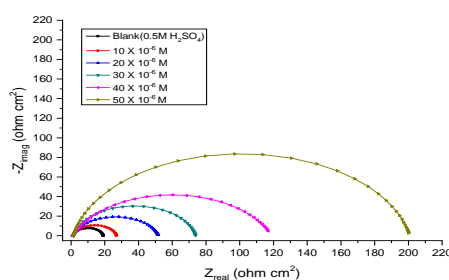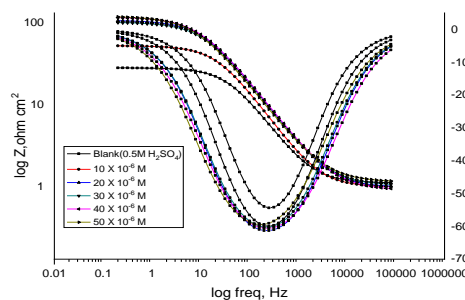

Fig 17. Bode plots for the dissolution of CS in half molar of H_2SO_4 in the existence and non-existence of various concentration of compound (B) at 25 ^{o}C.

Table 7 .EIS for CS corrosion in existence and non-existence of altered doses of different organic compounds at 25^oC.

Compound	[Inh] M	R_{ct} (Ωcm^2)	C_{dl} (μFcm^{-2})	θ	%IE
Blank	0.5	10.36	206.3	--	--
A	10×10^{-6}	81	86	0.872	87.2
	20×10^{-6}	88.3	72.4	0.883	88.3
	30×10^{-6}	104	63.4	0.90	90
	40×10^{-6}	110.6	55.3	0.906	90.6
	50×10^{-6}	122	54.2	0.915	91.5
B	10×10^{-6}	158	47	0.934	93.4
	20×10^{-6}	170	42	0.939	93.9
	30×10^{-6}	182	36	0.943	94.3
	40×10^{-6}	210	28	0.951	95.1
	50×10^{-6}	260	24	0.96	96

3.3. Techniques for Surface Examinations

3.1. FT-IR method:

There is a slightly shift in the peaks of the inhibitor function groups which adsorbed on the CS surface and this indicate that these compounds can act as corrosion inhibitor as in Figure (18 &19)[17-18].
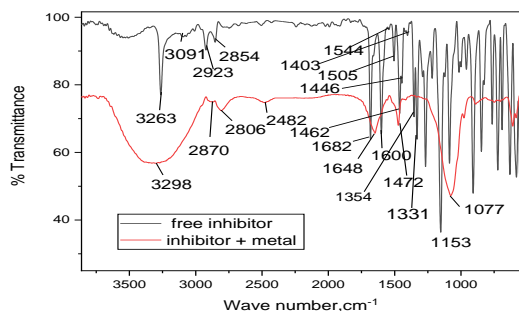

Fig.19. FT-IR spectrum of compoun(A) before and after adsorption on CS surface
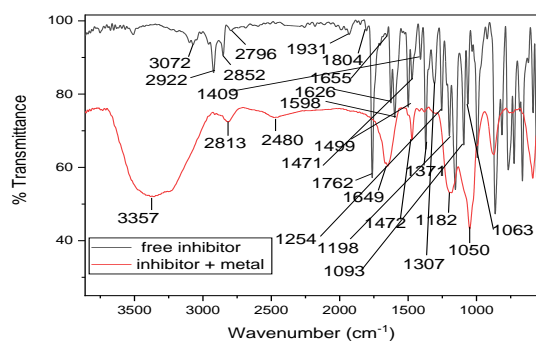

Fig.20. FT-IR spectrum of compound (B) before and after adsorption on CS surface.

3.5. Corrosion Inhibition Mechanism

The study detected that the adsorption is physical adsorption and the adsorbed molecule form a coated layer on CS to inhibit its corrosion. The SO_4^{2-} ions get adsorbed on CS surface and turn it as negatively charged surface, the protonated inhibitors molecules (cationic) get adsorbed on the negatively charged of CS by an electrostatic attraction .The protonated molecules could adsorb on the CS surface of the specimen[19-25].

4. References:

1 Tan, B., Zhang, S., Cao, X., Fu, A., Guo, L., Marzouki, R., & Li, W. (2022). Insight into the anti-corrosion performance of two food flavors as eco-friendly and ultra-high performance inhibitors for copper in sulfuric acid medium. *Journal of Colloid and Interface Science*, **609**, 838-851.

2 Kadhim, A., Betti, N., Al-Adili, A., Shaker, L. M., & Al-Amiery, A. A. (2022). Limits and developments in organic inhibitors for corrosion of mild steel: a critical review (Part two: 4-aminoantipyrine). *Int. J. Corros. Scale Inhib*, **11(1),** 43-63.

3 Xiao, J., Long, X., Qu, W., Li, L., Jiang, H., & Zhong, Z. (2022). Influence of sulfuric acid corrosion on concrete stress–strain relationship under uniaxial compression. Measurement, 187, 110318.

4 Haruna, K., Alhems, L. M., & Saleh, T. A. (2021). Graphene oxide grafted with dopamine as an efficient corrosion inhibitor for oil well acidizing environments. Surfaces and Interfaces, 24, 101046.

5 Ali, A. E., Badr, G. E., & Fouda, A. (2021). Citrus sinensis extract as a Green inhibitor for the corrosion of carbon steel in sulphuric acid solution. Biointerface Research in Applied Chemistry, **11(6)**, 14007-14020.

6 Abdel Hameed, R. S., Al-Bagawi, A. H., Shehata, H. A., Shamroukh, A. H., & Abdallah, M. (2020). Corrosion inhibition and adsorption properties of some heterocyclic derivatives on C-steel surface in HCl. *Journal of Bio-and Tribo-Corrosion*, **6(2),** 1-11.

7 Suhasaria, A., Murmu, M., Satpati, S., Banerjee, P., & Sukul, D. (2020). Bis-benzothiazoles as efficient corrosion inhibitors for mild steel in aqueous HCl: molecular structure-reactivity correlation study. *Journal of Molecular Liquids*, *313*, 113537.

8 Acharya, M. G., & Shetty, A. N. (2019). The corrosion behavior of AZ31 alloy in chloride and sulfate media–a comparative study through electrochemical investigations. *Journal of Magnesium and Alloys*, **7(1),** 98-112.

9 El-Katori, E. E., & Al-Mhyawi, S. (2019). Assessment of the Bassia muricata extract as a green corrosion inhibitor for aluminum in acidic solution. *Green chemistry letters and Reviews*, **12(1),** 31-48.

10 Fouda, A. S., Eissa, M., & El-Hossiany, A. (2018). Ciprofloxacin as eco-friendly

corrosion inhibitor for carbon steel in hydrochloric acid solution. *Int. J. Electrochem. Sci*, *13*, 11096-11112.

11 Abdallah, M., Altass, H. M., Al-Gorair, A. S., Al-Fahemi, J. H., Jahdaly, B. A. A. L., & Soliman, K. A. (2021). Natural nutmeg oil as a green corrosion inhibitor for carbon steel in 1.0 M HCl solution: Chemical, electrochemical, and computational methods. *Journal of Molecular Liquids*, *323*, 115036.

12 Shahzad, K., Sliem, M. H., Shakoor, R. A., Radwan, A. B., Kahraman, R., Umer, M. A., & Abdullah, A. M. (2020). Electrochemical and thermodynamic study on the corrosion performance of API X120 steel in 3.5% NaCl solution. Scientific reports, **10(1),** 1-15.

13 Gharbi, O., Tran, M. T., Tribollet, B., Turmine, M., & Vivier, V. (2020). Revisiting cyclic voltammetry and electrochemical impedance spectroscopy analysis for capacitance measurements. Electrochimica Acta, 343, 136109.

14 Meddings, N., Heinrich, M., Overney, F., Lee, J. S., Ruiz, V., Napolitano, E., ... & Park, J. (2020). Application of electrochemical impedance spectroscopy to commercial Li-ion cells: A review. *Journal of Power Sources*, **480**, 228742.

15 Kwiecien, M., Badeda, J., Huck, M., Komut, K., Duman, D., & Sauer, D. U. (2018). Determination of SoH of lead-acid batteries by electrochemical impedance spectroscopy. Applied Sciences, *8*(6), 873.

16 Hoshi, Y., Koike, T., Tokieda, H., Shitanda, I., Itagaki, M., & Kato, Y. (2019). Non-contact measurement to detect steel rebar corrosion in reinforced concrete by electrochemical impedance spectroscopy. *Journal of The Electrochemical Society*, **166(11),** C3316.

17 Gao, F., Wang, J., Zhang, H., Jia, H., Cui, Z., & Yang, G. (2018). Role of ionic strength on protein fouling during ultrafiltration by synchronized UV–vis spectroscopy and electrochemical impedance spectroscopy. *Journal of Membrane Science*, **563**, 592-601.

18- Ouakki, M., Galai, M., Benzekri, Z., Verma, C., Ech-chihbi, E., Kaya, S. A. V. A. Ş., ... & Cherkaoui, M. (2021). Insights into corrosion inhibition mechanism of mild steel in 1 M HCl solution by quinoxaline derivatives: electrochemical, SEM/EDAX, UV-visible, FT-IR and theoretical approaches. *Colloids and Surfaces A: Physicochemical and Engineering Aspects, 611, 125810.*

19 Albrakaty, R. H., Wazzan, N. A., & Obot, I. B. (2018). Theoretical study of the mechanism of corrosion inhibition of carbon steel in acidic solution by 2-aminobenzothaizole and 2-mercatobenzothiazole. *Int. J. Electrochem. Sci*, **13**(4), 3535-3554.

20 Pareek, S., Jain, D., Hussain, S., Biswas, A., Shrivastava, R., Parida, S. K., ... & Behera, D. (2019). A new insight into corrosion inhibition mechanism of copper in aerated 3.5 wt.% NaCl solution by eco-friendly Imidazopyrimidine Dye: experimental and theoretical approach. *Chemical Engineering Journal*, *358*, 725-742.

21 Obot, I. B., Haruna, K., & Saleh, T. A. (2019). Atomistic simulation: a unique and powerful computational tool for corrosion inhibition research. *Arabian Journal for Science and Engineering*, **44(1),** 1-32.

22 Liu, Z., Ye, Y. W., & Chen, H. (2020). Corrosion inhibition behavior and mechanism of N-doped carbon dots for metal in acid environment. *Journal of Cleaner Production*, *270*, 122458.

23 Zhou, J., Niu, X., Cui, Y., Wang, Z., Wang, J., & Wang, R. (2020). Study on the film forming mechanism, corrosion inhibition effect and synergistic action of two different inhibitors on copper surface chemical mechanical polishing for GLSI. Applied Surface Science, 505, 144507.

24 Paul, P. K., & Yadav, M. (2020). Investigation on corrosion inhibition and adsorption mechanism of triazine-thiourea derivatives at mild steel/HCl solution interface: Electrochemical, XPS, DFT and Monte Carlo simulation approach. *Journal*

of *Electroanalytical Chemistry*, *877*, 114599.

25 Guo, L., Tan, J., Kaya, S., Leng, S., Li, Q., & Zhang, F. (2020). Multidimensional insights into the corrosion inhibition of 3, 3-dithiodipropionic acid on Q235 steel in H2SO4 medium: a combined experimental and in silico investigation. *Journal of colloid and interface science*, **570**, 116-124.